



# Behaviour of Backfill Undergoing Cementation Under Cyclic Loading

Imad Alainachi · Mamadou Fall · Muslim Majeed

Received: 20 December 2020 / Accepted: 11 May 2022 / Published online: 9 June 2022  
© The Author(s), under exclusive licence to Springer Nature Switzerland AG 2022

**Abstract** Cemented paste backfill (CPB), a man-made soil undergoing cementation, is extensively applied to support underground mine openings or spaces and provide regional ground stability. The large underground cavities created by the ore extraction are backfilled with the tailings (fine-grained soils) mixed with cement and water in the form of CPB. Cyclic loading-induced liquefaction potential of CPB structures is a crucial concern in underground mine workplaces and backfilling operations. Failures of CPB structures can cause loss of life and/or serious injuries and have significant financial ramifications for a mine. However, no studies have used the shaking table testing method to address the cyclic and liquefaction response of CPB undergoing hydration. This research highlights new findings of using a shaking table to understand the effect of the progress of cement hydration (curing time) on the geotechnical response of hydrating CPB during dynamic loading events. CPB blends were produced, casted into a flexible laminar shear box and kept for curing to different maturity ages. Various factors (e.g., horizontal and vertical deformation, development of excess pore water pressure, temperature, electrical conductivity, acceleration, effective stress) were monitored before, during, and after shaking. Microstructural evolution of

CPB was also studied. Cyclic loading was applied using a 1-D shaking table. The findings indicate that the maturity age or the cement hydration development and the depth in the CPB have a significant influence on the acceleration and excess pore water pressure (PWP), as well as on the horizontal and vertical deformation of the CPB when subjected to cyclic loading. It is also found that the cyclic loading has an insignificant effect on the progress of the cementation hydration. Furthermore, young (2.5 h old) CPB material can be susceptible to liquefaction, whereas older CPBs (curing time  $\geq 4$  h) are resistant to liquefaction under the studied cyclic conditions. These results provide a better comprehension of cyclic behavior of natural or man-made soil undergoing cementation and the efficient and safer design of CPB structures. This will contribute to increase the safety of the underground mine openings and workplaces.

**Keywords** Liquefaction · Cyclic loading · Shaking table · Cemented paste backfill · Tailings · Cement hydration · Mine

## 1 Introduction

Mining has significantly contributed to the economy and effectively impacted the development of several regions and countries around the world. In Ontario (Canada), for instance, mining produces around \$10

---

I. Alainachi · M. Fall (✉) · M. Majeed  
Department of Civil Engineering, University of Ottawa,  
161 Colonel by, Ottawa, ON K1N 6N5, Canada  
e-mail: mfall@uottawa.ca

billion of revenues every year (Dungca et al. 2006; Ontario Mining Association 2017). However, it is known that mine ore extraction activities have a negative impact on the environment as they produce huge quantities of solid waste (e.g., tailings). The surface disposal or management of these tailings was found to be a potential source of environmental (e.g., generation of acid mine drainage) and geotechnical (e.g., tailings dam failure) hazards. Moreover, the extraction of mine ores leads to the formation of large underground openings, which may cause ground subsidence and/or many other geotechnical engineering problems in the mine and the nearby areas. Furthermore, the instability of these underground openings (stopes) can jeopardize the safety of the mining workplace and the surrounding public agglomeration (Kesimal et al. 2005; Jamali 2012; Cui and Fall 2015).

To enhance the stability of these mine stopes or underground openings, and to guarantee the protection of the people in the mine and its adjacent areas as well as to manage the aforementioned mine wastes (tailings) in a safer and more environmental friendly way, a mixture (named cemented paste backfill, CPB) of tailings (predominantly made of silt-size particles), water and binder has been extensively used over the past few decades as the main supporting agent in underground mining operations and as a novel tailings management method around the world (Fall et al. 2005; Saebimoghaddam 2010; Abdul-Hussain and Fall 2012). Geotechnically, CPB is viewed as a cementing fine-grained soil.

The typical CPB mixture is prepared with tailings (70–85wt%), hydraulic binder (3–8%; often) agent (such as fly ash, slag, or cement) and water (fresh or mine processed). These ingredients are mixed in paste backfill production facility commonly situated on the mine surface and then pumped into the mine stope (Fall et al. 2010; Yilmaz et al. 2015). Adopting CPB in mine stopes backfilling is today a common practice in many mines worldwide, because it can be prepared and distributed in the mine stope in a relatively rapid time. This allows the backfilling process to be completed in a matter of days, compared to previous backfilling methods that could take weeks or months. Besides binder cost saving, decreasing stope cycle time helps generating additional revenue (Fall et al. 2008; Thompson et al. 2009).

However, young CPB built in an underground mine stope has been shown to be vulnerable to different geotechnical engineering problems (e.g., mechanical instability), when exposed to static loadings, as well as liquefaction, when exposed to dynamic loadings, such as seismic events or blast loadings. Failure of CPB in mine stopes may cause loss of life and/or serious injuries to mine workers, in addition to significant economic consequences for the mine and its related operations (Poulos et al. 1985; Fall et al. 2010; Becker et al. 2014). Thus, studying the mechanical stability of young CPB structures under static loading conditions and cyclic-induced liquefaction of CPB material at an early age is useful for efficient and safer design of CPB structures.

Most of the earlier studies on mechanical stability of young CPB focused on static loading conditions (e.g., Nasir and Fall 2010; Li and Aubertin 2012; Wu et al. 2014; Ghirian and Fall 2016; Fang and Fall 2020). There is a paucity of studies (Lu and Fall 2017; Saebimoghaddam 2010) on the liquefaction response of fresh CPB material under dynamic loading conditions, particularly cyclic loadings. There is a need to increase our understanding of the cyclic response and liquefaction potential of early age CPB since seismicity is common in underground mining activities.

CPB structures in underground mine cavities can be exposed to various sources of cyclic loadings. These cyclic loadings can originate from natural earthquake or commonly from mining-induced seismic events. There are various types of cyclic events that can occur as a result of mining activities, including fault slip (earthquake), rockburst, bump, pillar burst and outburst, pillar punching, disruption of geological features (Hasegawa et al. 1989). Moreover, the frequency of occurrence and seriousness of mine-induced cyclic events tend to rise with a growing depth of mine and volume of ore extraction (Hasegawa et al. 2009). Thus, the gradual reduction of ore existing at shallow depths in many underground mines in several regions in combination with a growing rate of volume extraction indicates that underground mining operations are more and more being accomplished at greater depths and with larger volume, and thus at higher magnitude and/or recurrent seismic events. This would suggest that CPB structures will be increasingly subjected to more frequent and severe cyclic loadings, which could increase the risk of liquefaction susceptibility in CPB structures at early ages. There is a mutual consent that

earthquake characteristics, such as peak ground acceleration and shaking time (number of loading cycles) significantly affect the behavior of liquefiable material (Carter 1988). It was also found that soil might liquefy if it was exposed to an earthquake of peak ground acceleration as low as 0.05 g (James et al. 2003). It should also be noted that exposure of soils (natural or artificial) to dynamic loads (e.g., vibration) results in the early rearrangement and settlement of soil particles, which can lead to densification (compaction) of the soil. This behavior has led to the development and application of soil dynamics improvement techniques in several locations around the world (Anastasopoulos et al. 2010; Plewes et al. 2010). Therefore, exposure of a fresh cementitious material (e.g., fresh concrete, fresh CPB) to vibrations during pouring, could lead to densification of the cementitious material, thereby improving its solidification (Sudarshan and Chandrashekar Rao 2017). However, due to the presence of high water content in CPB, exposure of this material to dynamic/cyclic loading could lead to liquefaction (Porcino et al. 2015).

A shaking table has been commonly used in engineering practice to study and understand the behavior of geomaterials and engineering structures when exposed to cyclic or seismic loadings for many decades despite its limitations (e.g., in situ stress simulation difficulty, high cost) (Moncarz and Krawinkler 1981; Ngadimon 2006; Su et al. 2020). The extensive utilization of shaking table experiments in geotechnical engineering studies is due to its facility to adopt different testing conditions. For instance, a shaking table can function either in one direction or multi directions of loading input, and the user is able to control and measure the cyclic load factors (amplitude and frequency). Also, it can be conducted on many types of soil under different saturation conditions (dry, unsaturated or saturated). In the past decades, numerous shaking table tests were carried out to evaluate the liquefaction response of natural soils during seismic events (Bairro and Vaz 2000; Ueng et al. 2006; Mohamed 2014; Guoxing et al. 2015; Wang et al. 2015; Zhend and Yue 2020), whereas only limited studies were carried out to understand the dynamic response of tailings (non-cemented) by using shaking tables (James et al. 2003; Pépin et al. 2009, 2012b; Özgen et al. 2011). These studies have significantly contributed to understanding the response of natural

soils and/or uncemented tailings during cyclic events. Previous studies by the authors (e.g., Alainachi and Fall 2021a, b) have used the shaking table to study the cyclic behavior of 4-h old-CPB fresh material (i.e. CPB with a constant age) under different conditions, such as the variation of mixing and curing temperature and the presence of uncontrolled chemical components. However, no studies have been carried out by using a shaking table to assess the effect of maturity (curing time), and thus, the effect of the progress of cement hydration, on the dynamic or liquefaction response of cemented tailings exposed to cyclic loadings at early ages. It is therefore essential to address this knowledge gap because, in the field, the age of the CPB structure changes over time and the CPB is subject to cement hydration processes that alter its geotechnical response and properties over time. Accordingly, the goal of this research is to use the shaking table technique to study the effect of the progress of cement hydration (curing time) on the geotechnical behavior and liquefaction potential of hydrating cemented paste backfill material at early ages when subjected to cyclic loadings.

## 2 Experimental Materials and Apparatus

### 2.1 Materials

The main ingredient of CPB mixture tested in this research was Silica Tailings (ST), which is synthetic tailings material that is made of ground silica. The grain size distribution of (ST) is similar to the average grain size distribution of various tailings that were extracted from nine different Eastern Canadian mines (9MT), as shown in Fig. 1. Minerals of ST are principally constituted of quartz, which is the predominant mineral in hard rock mine tailings in Canada. ST contains a percentage of as high as 99.8% SiO<sub>2</sub> of silica, which makes it a chemically inert material. Accordingly, silica tailings were selected in this research in order to minimize the uncertainties that might occur when using natural tailings to the lowest level by reducing or controlling the possible chemical reaction of the tailings with other components in the CPB blend (Carraro et al. 2009; Aldhafeeri and Fall 2016; Haiqiang et al. 2016). Figure 1 and Table 1 illustrates the physical properties of ST that is used in this study.

**Fig. 1** Average grain size distribution of tailings extracted from nine Canadian mines (9MT) vs the grain size distribution of the silica tailing (ST)

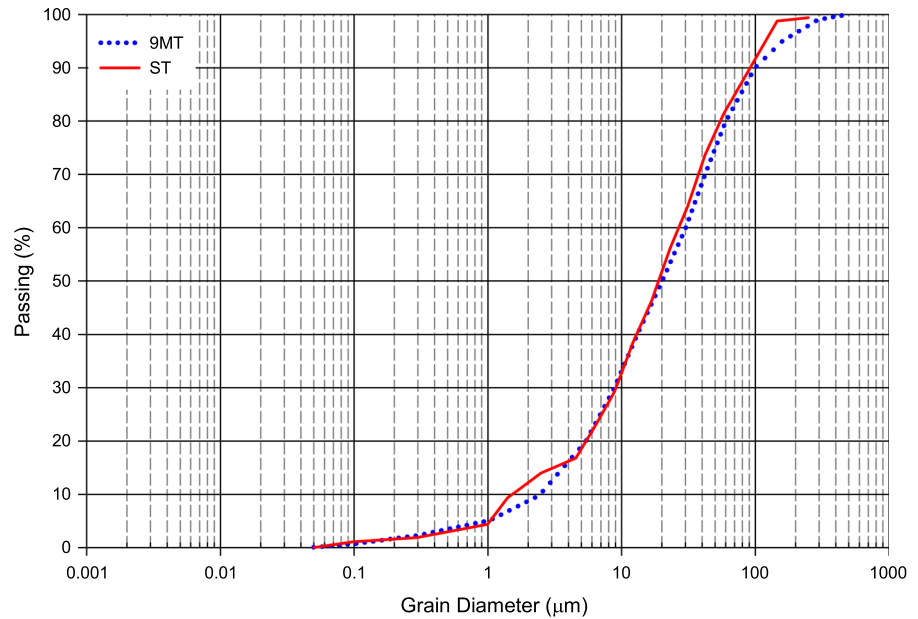


**Table 1** Primary physical properties of the tailings

Tailings	Gs	D <sub>10</sub> (μm)	D <sub>30</sub> (μm)	D <sub>50</sub> (μm)	D <sub>60</sub> (μm)
ST	2.7	1.9	9.0	22.5	31.5

Adequate amounts of hydraulic binder are typically blended with tailings and water in order to improve the mechanical properties of CPB. The hydraulic binder agent used in this research was Portland cement type I (PCI) (Table 2), as it is the most common binder used in preparing CPB around the world. Mixtures were prepared using tap water as mixing water.

## 2.2 Paste Backfill Mixture Preparation

CPB samples were prepared by blending tailings with 4.5 wt% of PCI, and water with a water-cement ratio (w/c) of 7.6. To obtain a homogenous paste, samples were blended for 10 min. The prepared backfill

mixture was prepared with 18 cm of slump, which is one of the most common slump values used in the Canadian mines in their paste backfill operations. The slump test procedure in this research followed the ASTM C143/C143M-15a (2015). The CPB blend was prepared with degree of saturation (S) 100%.

Afterward, CPB blends were casted into the manufactured laminar shear box (described below). The laminar box containing CPB mixtures was sealed to eliminate changes in water content due to evaporation and kept for curing in a temperature-controlled room (~ 25 °C) until reaching the testing ages according to the testing program explained in Sect. 3.

## 2.3 Shaking Table

The shaking table, designed and manufactured at the university of Ottawa (Fig. 2), was used in this research to simulate the motion of the tested CPB when subjected to a seismic or cyclic event. This shaking table consists of a ~ 1200 × ~ 1060 mm platform,

**Table 2** Primary physical and chemical properties of the Portland cement type I (PCI)

Gs	SSA <sup>a</sup> (m <sup>2</sup> /g)	S (wt%)	Ca (wt%)	Si (wt%)	Al (wt%)	Mg (wt%)	Fe (wt%)	Si/Ca
3.15	1.32	1.5	44.9	8.4	2.4	1.6	1.9	0.2

<sup>a</sup>Specific surface area

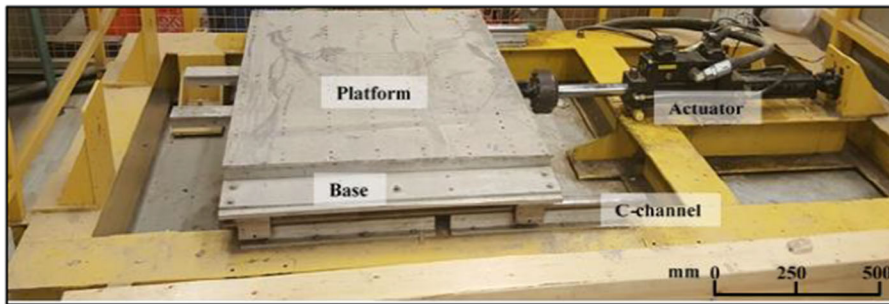


**Fig. 2** Shaking table used in this study

a steel base, and steel C-channels between them. This table provides a series of longitudinal (1-D) sinusoidal cyclic motions with one degree of freedom of horizontal displacement. This shaking table is driven by a hydraulic actuator and runs in the range of 1–17 Hz. The displacement limit of this table is 120 mm, and the maximum base shear capacity is 27 kN (Mohamed 2014).

In order to use the shaking table to study the cyclic behavior of CPB, a Flexible Laminar Shear Box (FLSB) was manufactured at the Faculty of Engineering of the University of Ottawa solely for this research (Fig. 3). The Flexible Laminar Shear Box consists of 30 horizontal laminas. The inner dimension of each lamina is 75 × 75 cm, and the total capacity of assembled box is 75 × 75 cm (in plan) and 100 cm (in depth). The laminas are made of 3.2 × 3.2 cm aluminum alloy box sections. The FLSB was manufactured with a 2 mm clearance



**Fig. 3** Flexible Laminar Shear Box (FLSB) developed and built for this study

spacing between laminas to warrant the movement independency of each lamina. To contain/hold the CPB mixture, a flexible membrane (made of polyethylene) was placed inside the FLSB. This membrane has a high flexibility with a thickness of as low as 0.5 mm, which provides no (or negligible) effect on the movement of the FLSB (Mohamed 2014). The FLSB and the membrane were securely fixed to the platform of the shaking table, and the prepared CPB blend was then poured inside the FLSB. The dimension of the CPB sample to be tested was 75 × 75 × 75 cm.

Various sensors or transducers were installed at various levels in the sample (the FLSB with its content) as shown in Fig. 4A and B and explained below:

### 2.3.1 Vertical Displacements Transducers: (Item 1 in Fig. 4)

- a. Linear variable differential transformer (LVDT) to determine the surficial vertical displacement of the CPB sample. HCD-1000 LVDTs with a range of 2.5 cm were used in this regard
- b. Cable transducers (CTs) to monitor the vertical displacement at various depths (20 cm, 40 cm and 60 cm). Each CT was securely fixed to a combination of a thin metal rod connected to lightweight, perforated plastic plates of 2 cm (L) × 2 cm (W) × 2 cm (Thickness) dimensions, which were perforated to eliminate the seepage pressure induced movement. CTs combinations were installed at three different levels within each specimen. To eliminate uncontrolled tilting and/or displacement during the shaking, these combinations were placed within cylindrical

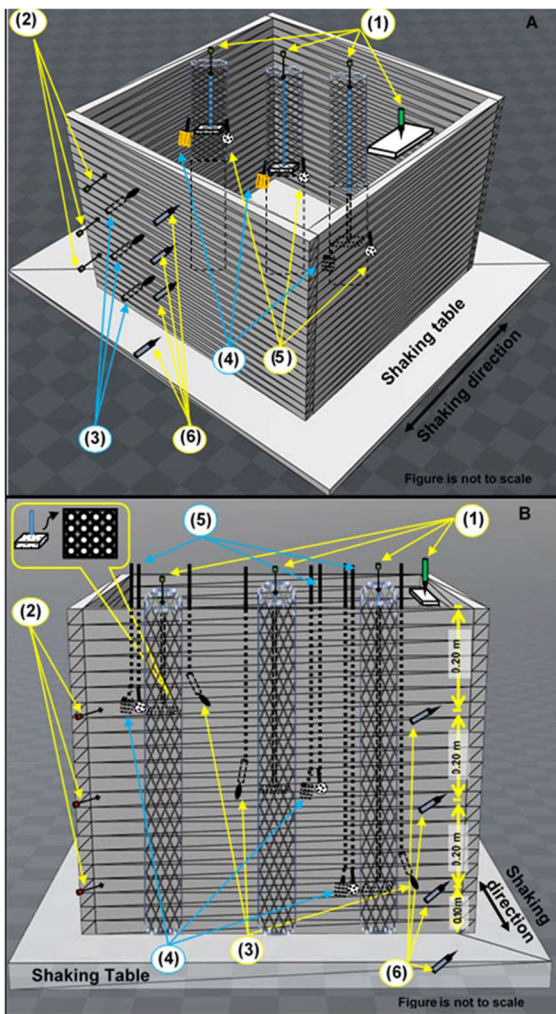


**Fig. 4** Schematic view of the FLSB and instruments locations **A** 3D Sketch, **B** 2D Sketch. (1) Vertical displacement transducers, (2) Horizontal displacement transducers, (3) P.W.P. transducers, (4) VWC/EC/Temp. sensors (5) Suction sensors, and (6) Accelerometers

guidance towers that were made of thin metal mesh sheets. These towers were securely fixed to the platform of the shaking table (Fig. 5) to allow the whole system to follow the same motion rhythm and to avoid being a supporting factor. Celesco SP2-12 compact string transducers were used in this regard. The measurement range of this transducer is around 32 cm.

**Horizontal displacement (HD) transducers** Cable transducers (CT) to determine the horizontal displacement of the CPB sample at the levels of 20 cm, 40 cm and 60 cm. CTs were attached to the outside of the

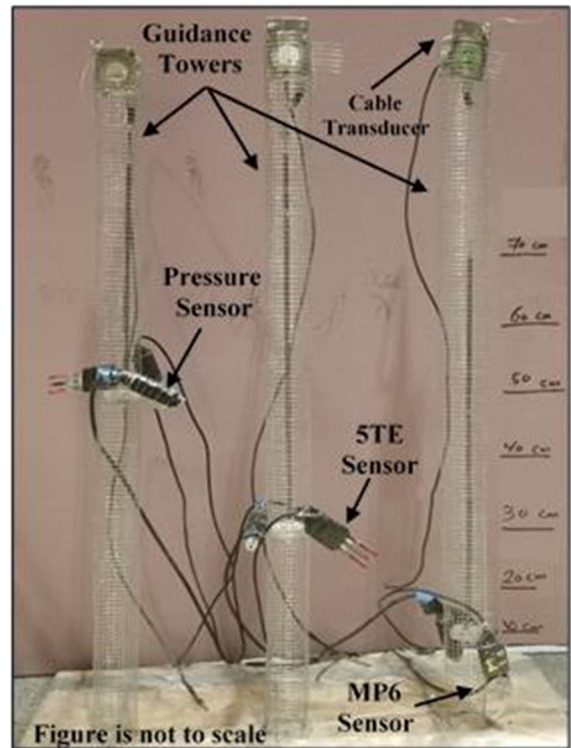


**Fig. 5** Guidance towers and related instrumentation setup

FLSB at the depth-related laminas (Item 2 in Fig. 4). The same type of transducers as in (a) were used in this regard.

**P.W.P transducers** To determine the dynamic load-induced changes in pore-water pressure, pressure transducers were placed at the levels of 20 cm, 40 cm and 60 cm of each specimen inside the FLSB (Item 3 in Fig. 4). PX309 series pressure transducers were used in this regard. The range and static accuracy of these transducers are  $-15$  to  $+15$  PSI and  $\pm 0.25\%$ , respectively.

**VWC/EC/Temp. sensors** ECH2-5TE sensors were used to determine the variation in the volumetric water content (VWC), electrical conductivity (EC), and temperature. The range of volumetric water content (VWC) that this sensor measures is 0–80% with the accuracy of  $\pm 0.01$  from 1 to 40% and the accuracy of  $\pm 0.15$  from 40 to 80%. The range and accuracy of electrical conductivity (EC) that can be monitored with this sensor is 0–23 dS/m and  $\pm 0.1$ , respectively. The accuracy of temperature measurement of this sensor is  $\pm 1$  °C. In this regard, these sensors were placed at the levels of 20 cm, 40 cm and 60 cm within

each sample (Item 4 in Fig. 4). Changes in EC give info about the rate of the water-cement chemical reactions resulting from ion migration. Monitoring EC is a powerful method to evaluate the development of cement hydration and the related changes of the material structure (Li and Fall 2016). By monitoring VWC, the water flow in the CPB mass can be determined and the self-dehydration of CPB (consumption of capillary water by cement hydration) can be assessed. Temperature variation monitoring provides valuable evidence about the cement hydration progress.

**Suction sensors** To record/monitor the time histories of suction development during the CPB curing period, section sensors were used and placed at various levels (20 cm, 40 cm and 60 cm) within each specimen (Item 5 in Fig. 4). In this study, water suction potential was determined using the ECH2-MPS6 sensors (Dielectric water potential sensors). This sensor measures suction at the range of  $-9$  to  $-100,000$  kPa with a resolution of 0.1 kPa, and reading accuracy of  $\pm 10\%$ .

**Accelerometers** To measure/maintain the shaking acceleration, four accelerometers were used in this study (Item 6 in Fig. 4); one was connected to the shaking table and three accelerometers were connected to the outside of the FLSB at different depths (20 cm, 40 cm and 60 cm). Endeeco – 7593A transducers were used in this study. The frequency response of these transducers is 0–50 Hz, and the full-scale range is  $\pm 2$  g.

To eliminate any displacement of the pressure transducers, 5TE and MPS6 sensors, they were all attached to the guidance towers. VD transducers, HD transducers, P.W.P. transducers and accelerometers were connected to signal conditioning and Data Acquisition Systems (DAQS). Also, 5TE and MPS6 sensors were connected to Decagon Em50 series data loggers. DAQS and Em50 were connected to a computer to record and analyze the required data. The data collection interval was 1 s during shaking and 10 min. before and after shaking. Moreover, each step of the testing program (mixing, installation and shaking operation) was recorded using a high definition digital camera.

### 3 Program and Procedure of Experimental Test

It should be emphasized that the main purpose of the experimental program is to assess the effect of the progress of cement hydration on the response of CPB material under cyclic loading. The objective is not to use the shaking table testing technique to assess the response of hydrating CPB structure when subjected to cyclic loading. Using shaking table testing technique to simulate the seismic behavior of a CPB structure that can be as high as 150 m requires an unrealistic costly approach of using of a shaking table testing instrument of very large-scale to reflect the full size (or a reasonable height) of the CPB structure and/or its complex in situ stress, or to accurately scale down the experiment parameters based on the laws of similarity. However, consideration of full field scale prototype model does not ensure that all or key factors meet the similitude laws in the 1-g gravity field, because the CPB structures might be subjected to complex field loadings conditions. Hence, this experimental program was designed to assess the response of the backfill material undergoing cementation during shaking. In other words, a backfill height of 0.70 m (micro-prototype) was considered. Though the CPB material (not CPB structure) was assessed in this research, gaining insight into the behavior of cemented backfill material exposed to seismic loads will allow to understand the cyclic response of CPB structure as well as establish future constitutive models to describe the cyclic response of hydrating CPB. Moreover, considering a CPB micro-prototype will allow to satisfy the key requirements of similarity between the prototype and the physical model. Accordingly, a 1:1 geometric scaling factor (N) was implemented for experimental shaking table tests on the scale model in this study. The geometry and configuration of models were designed based on the similarity theories related to the 1 g shaking table test for the soil-fluid models proposed by Iai (1989) and Meymand (1998). The summary of the experimental testing program that was conducted in this study is shown in Fig. 6 and Table 3 and described below.

**Fig. 6** Flow chart of the experimental program and testing conditions

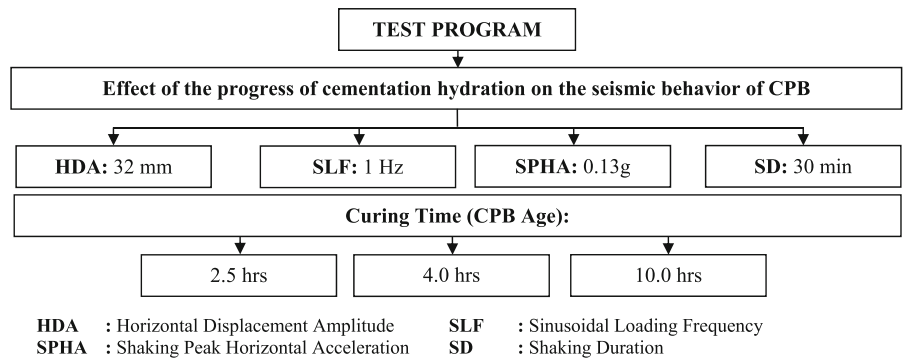


**Table 3** Summary of the testing program

Test	Material	Age (hrs)	HDA (mm)	SLF (Hz)	SPHA	SD (min)	PLMD (hrs)
1	CPB	2.5	32	1	0.13 g	30	24
2	CPB	4	32	1	0.13 g	30	24
3	CPB	10	32	1	0.13 g	30	24

*HDA*: Horizontal Displacement Amplitude, *SLF*: Sinusoidal Loading Frequency, *SPHA*: Shaking Peak Horizontal Acceleration, *SD*: Shaking Duration, *PLMD*: Post Loading Monitoring Duration

### 3.1 Shaking Table

#### 3.1.1 Test Conditions and Cyclic Parameters

Prior to conducting a shaking table test, the test conditions, as well as the cyclic/seismic parameters need to be determined in order to simulate a cyclic event. These parameters include Shaking Peak Horizontal Acceleration (SPHA), Sinusoidal Loading Frequency (SLF), Shaking Duration (SD), and Horizontal Displacement Amplitude. Due to limitations of this experiment (e.g., the sensitivity and/or limitation of the monitoring sensors and transducers used in this experiment, as well as the shaking table maximum capacity), some values of these parameters were altered to consider these limitations, although they might not simulate the actual situation of a cyclic event. However, this type of procedure is often used in liquefaction related studies (Ishihara 1996). Hence, shaking table tests were carried out in this study using a cyclic load that was applied in a one-dimensional signal, a uniform amplitude, and at constant frequency.

Sriskandakumar (2004) found that the frequency loading magnitude applied in laboratory cyclic tests under undrained loading has insignificant influence or

negligible on the dynamic behavior of the tested materials (undrained conditions were applied in the present study). Moreover, Srilatha et al. (2013) concluded that the cyclic response of tested material is almost similar at frequencies less than 7 Hz. Thus, shaking table tests were conducted in this study using a sinusoidal loading of 1 Hz frequency.

On the one hand, the strongest ground motion related to mining events in northeastern Ontario (Canada) was recorded in 2006 with a value of 0.0027 g (Atkinson et al. 2008; Saebimoghaddam 2010; Natural Resources Canada 2019). On the other hand, the Saguenay earthquake 1988 in Quebec (Canada) was recorded to have a ground peak acceleration (GPA) value of 0.13 g (Tuttle et al. 1990). Many studies indicated that tailings may liquefy when they are exposed to a ground motion with horizontal GPA that exceeds 0.05 g (Carter 1988; James et al. 2003). Hence, the GPA in this study was selected to be equal to the GPA of the Saguenay earthquake 1988 in Quebec. It should be emphasized that the peak acceleration is the only parameter that matches to the GPA of Saguenay Earthquake, not the whole time series.

The maximum displacement of the simulator (deformation amplitude) can be determined using



Eq. 1 (Douglas 2003; Chopra 2005), which is based on peak ground acceleration and the values of loading frequency. Thus, the displacement amplitude used in the tests conducted in this study was calculated to be 32 mm.

$$a = [2\pi \times (1/T)]^2 \cdot A \quad (1)$$

where  $a$  and  $A$  are the peak ground acceleration and deformation (displacement) amplitude, respectively, and  $T$  is the loading cycle time (Douglas 2003; Chopra 2005).

Although recorded mine cyclic events (or earthquakes) do not last very long (Natural Resources Canada 2019), the shaking (cyclic event) applied in this study is carried out for 1800s (30 min) as shown in Table 4. This duration is not meant to represent the real duration of mine seismic events or earthquakes. The duration of 1800s was used to enable good examination of the seismic or cyclic behavior of the CPB samples and relative comparisons of their response, which is important for the future development of a constitutive model that can be used to describe the dynamic response of cemented soils or cemented tailings backfill. Moreover, according to Pépin et al. (2012b), who investigated the cyclic response of tailings (without cement) using a shaking table approach, the selected shaking duration depends on the material response towards liquefaction (reaching peak excess pore-water pressure). In their study, 1,000 s. was found to be a suitable shaking duration to reach cyclic peak of liquefaction of tailings without inclusions. They also found that another 1000 s of monitoring after shaking is required to obtain the full response of pore-water pressure dissipation. They also concluded that adding inclusions (e.g., blocks of

rocks) in tailings would reduce the development of excess pore-water pressure during shaking (to around 1700 s) and accelerate the excess pore-water pressure dissipation after loading. Accordingly, and as the material used in this study is tailings undergoing cementation (CPB mix), the duration of shaking was selected to range from 1 to 30 min (60–1800 cycles) depending on material response, and the post loading monitoring duration (PLMD) to continue (depending on material response) for additional 24 h.

### 3.1.2 Effect of the Progress of Cementation Hydration on the Cyclic Response of CPB

To assess the cyclic response of young CPB subjected to dynamic loadings, and to assess the effect of cementation hydration progress on this behavior, it was vital to apply dynamic (cyclic) loadings on CPB samples of various ages. Thus, CPB mixtures (poured in FLSB) were securely sealed and kept for curing under a stable temperature of 25 °C. Then, a series of shaking table tests were conducted on CPB models that were cured at various ages (see Fig. 6). It is important to note that the gradual formation of cement bonds between CPB particles usually occur during the early age of hydration. It was also found that the magnitude of cement hydration rapidly increases and reaches its peak in the period between 2 and 10 h after mixing (Bullard et al. 2011; Yilmaz et al. 2015). Accordingly, and to understand the effect of curing time on the cyclic behavior of CPB material, the shaking table tests were conducted on CPB samples that were cured at the ages of 2.5 h, 4.0 h, and 10.0 h.

**Table 4** Selected seismic parameters used in the present study and previous studies

Parameter	Values used in previous studies <sup>a</sup>	Values used in the present study
Horizontal displacement amplitude	10–80 (mm)	32 (mm)
Shaking peak horizontal acceleration	0.1 g–1.0 g	0.13 g
Sinusoidal loading frequency	0.1–50 (Hz)	1 (Hz)
Shaking duration <sup>b</sup>	3–2000 (s)	1800 (s)
Post loading monitoring duration	15 (min)–36 (h)	24 (h) <sup>c</sup>

<sup>a</sup>Such as (James et al. 2003; Ueng et al. 2006; Pépin et al. 2009, 2012a, b; Özgen et al. 2011; Mohamed 2014; Guoxing et al. 2015)

<sup>b</sup>Depends on the material response

<sup>c</sup>After initial casting

### 3.2 Microstructural Analysis

To understand the effect of microstructural evolution of CPB on its cyclic behavior, microstructural analyses were performed on cement paste samples of CPB cured at different ages. Microstructural analyses include X-ray diffraction (XRD) and thermal analysis (differential thermogravimetry (DTG), thermal gravimetry (TG)). Before conducting microstructural analysis, testing samples were first dried at 45 °C in a vacuum oven up to mass stabilization. Thermal analyses were performed using a TGA Q 5000 IR from TA Instruments. The different (dried) samples (about 20 mg each) were heated in an inert nitrogen atmosphere at the rate of 10 °C per minute up to a temperature of 1000 °C. The XRD tests were conducted using a Rigaku ultima IV diffractometer that is equipped with cross beam optics.

## 4 Results and Discussion

### 4.1 Acceleration and Horizontal Displacement

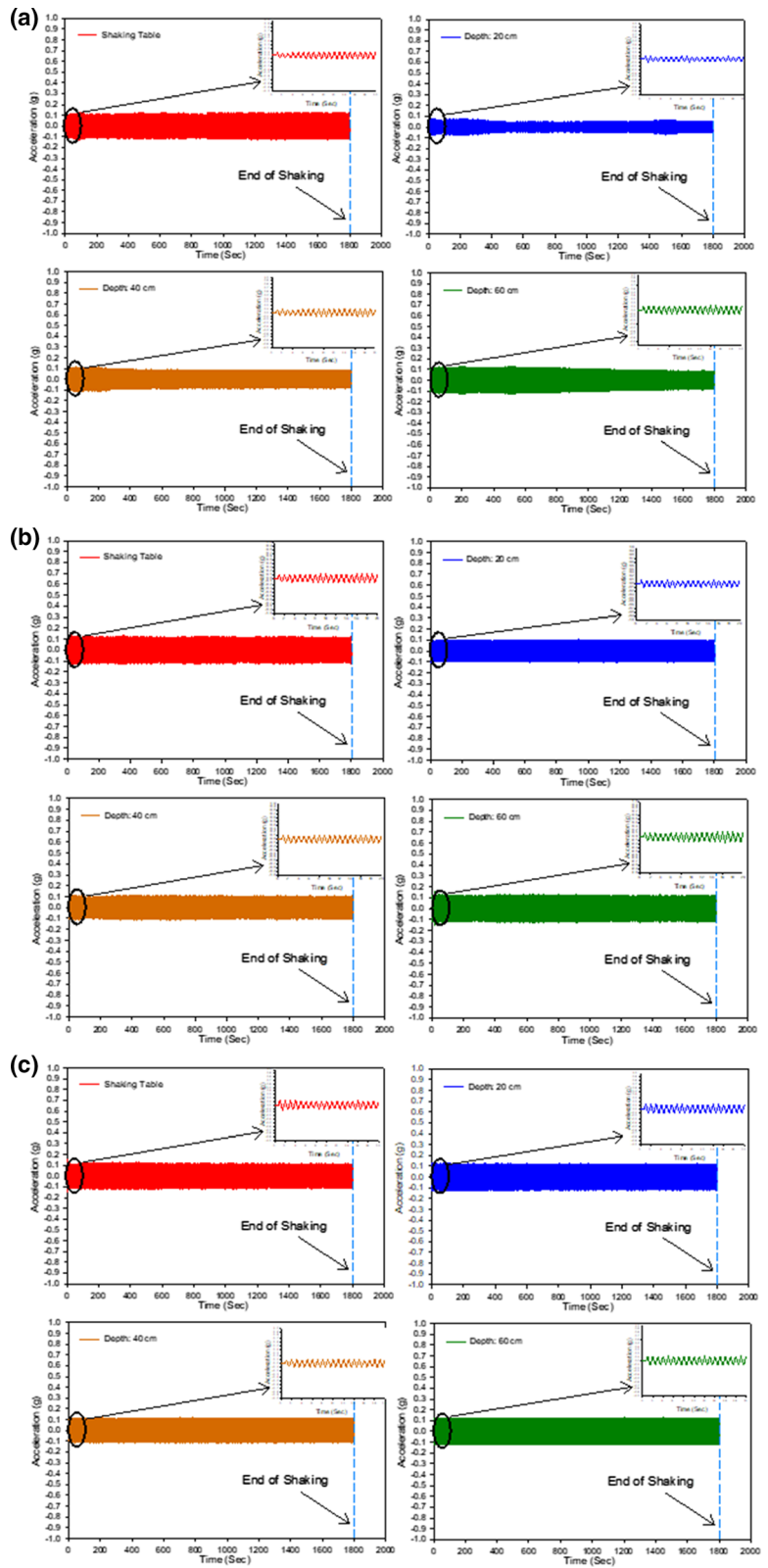
The acceleration and horizontal displacement (lateral deformation) results at various depths within each tested CPB sample are shown in this section with respect to curing time (which reflects the cementation degree). Combining the results of these two parameters can give an indication of the shear resistance of the tested material at various depths (Takahashi et al. 2001; Nouri et al. 2006, 2008).

### 4.2 Acceleration

Figure 7a–c shows the peak acceleration progress with time at various levels when shaking CPB models cured (aged) for 2.5 h, 4.0 h, and 10.0 h, respectively. This figure indicates that the maturity age or degree of cementation (the cement hydration progress) and the depth have an influence on the recorded acceleration values. CPB material cured for a longer time display higher values of peak acceleration comparing with CPB samples cured for a shorter time, which is more noticeable at shallow depths. The registered acceleration highly changed with depth for the models tested at early age (2.5 h), while the acceleration variation with depth was low and insignificant (negligible) for models tested at later ages: 4.0 h and 10.0 h,

respectively. For example, the peak acceleration of the CPB sample cured to 2.5 h (Fig. 7a) ranged from 0.10 to 0.125 g at 0.6 m depth (0.1 m above the shaking table), around 0.08–0.10 g at 0.4 m depth (0.3 m above the shaking table), as low as 0.04–0.08 g at 0.2 m depth (0.5 m above the shaking table). On the other hand, for the CPB model cured to 4.0 h, the peak acceleration (Fig. 7b) at depths 0.6 m, 0.4 m, and 0.2 m was noted to be around 0.115–0.125 g, 0.100–0.110 g, and 0.090–0.100 g, respectively. For the CPB model cured to 10.0 h, the peak acceleration at all depths was around 0.125–0.130 g. This reduction in the peak acceleration as the age or curing time of CPB decreases can be related to the influence of the cementation degree on the damping ratio. Previous studies (e.g., Acar and El-Tahir 1986; Yang and Woods 2015) have concluded that the (higher) degree of cementation reduces the damping ratio. This means that the CPBs cured for a longer curing time will have a lower damping ratio, since longer curing time is related to greater degree of cementation (degree of cement hydration) as evidenced by Figs. 17 and 18 and discussed later. The cement hydration progress strengthens the bonds between tailings (soil) grains and thus reduces the deformation level of the material (Mamlouk and Zaniewski 2011). The detected significant alteration (decrease) of the acceleration values with the diminution of the depth in the CPB cured for 2.5 h may be related to nonlinearity, and degradation of shear resistance and stiffness degradation of CPB because of liquefaction, as demonstrated by the liquefaction analysis results presented in Sect. 4.3. Excessive increase of the pore water pressure or liquefaction leads to a large deformation of the CPB cured for 2.5 h, in which the effect of cementation is not yet significant due to the lower cement hydration degree (see Figs. 17 and 18). The larger the deformation is, the greater the damage of the CPB pore structure. Moreover, the greater the dislocation and slip between the CPB particles (tailings, unreacted cement grains) are, the greater the friction between particles is, and the greater the material damping ratio would be; in other words, the greater would be the decrease of the acceleration value. This finding and explanation are consistent with the results of displacement monitoring as well as with the determination of effective stress and excess pore-water pressure ratio as discussed later. However, it should be mentioned that additional factors could have caused or contributed to

**Fig. 7** Measured peak acceleration histories at different depths vs time for CPB models cured to different times: **a** 2.5 h; **b** 4.0 h and **c** 10.0 h



the observed changes of acceleration with depth. These factors could be higher effect of excess pore pressure and reduction in damping ratio.

#### 4.2.1 Lateral (Horizontal) Displacement

Lateral (horizontal) displacement within liquefiable soils may refer to the deformation of the structure of these soils as a result of shaking-induced liquefaction. This tendency can be attributed to the fact that the ground vibration destabilizes the contact between soil particles, which will lead to a reduction of soil resistance against shaking (Takahashi et al. 2001; Dungca et al. 2006). Figure 8a–c shows the horizontal displacement at various depths during the cyclic loading times for CPB models cured (aged) for 2.5 h, 4.0 h, and 10.0 h, respectively.

Two key behaviours can be observed from these figures:

- (a) In all models, the horizontal displacement increased with the decrease in depth. This behavior is consistent with the conclusions of many past investigations (e.g., Motamed et al. 2013; Srilatha et al. 2013). This relationship can be attributed to the shaking-induced increase in material density due to the compaction (dynamic densification) of the tailings particles (Zhu and Clark 1994; Anastasopoulos et al. 2010). Nevertheless, the displacement variation with depth within the CPB model cured to 2.5 h was more significant than the variation in displacement with depth within the CPB model cured to 4.0 h. Moreover, there was a negligible displacement change with depth within the CPB model cured to 10.0 h. This reduction is related to the CPB solidification due to progress of the cement hydration with time. Longer curing means a generation of a larger amount of cement hydration products (e.g., C-S-H, CH), which in turn enhances the cohesion or degree of cementation of the CPB material (Fall et al. 2010; Yilmaz et al. 2015). This argument regarding the increase of cement hydration product with time is experimentally substantiated by the results of TG/DTG on cement pastes of CPB, which are presented (Figs. 17 and 18) and discussed later.

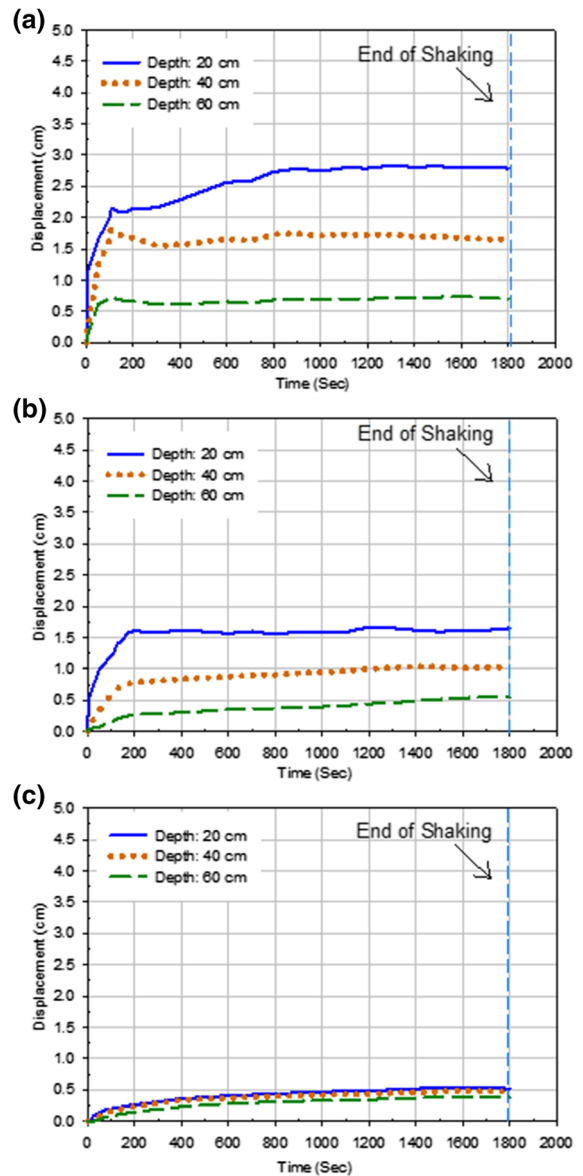


**Fig. 8** Lateral displacement histories at different depths vs times for CPB models cured to different times: **a** 2.5 h; **b** 4.0 h and **c** 10.0 h

- (b) The lateral displacement magnitude within the CPB model cured to 2.5 h was higher in value compared to the CPB model cured to 4.0 h, while there was low or insignificant lateral displacement within the CPB model cured to 10.0 h. This decrease of lateral displacement with progress of curing time is the result of the increase in bonds between the tailings particles with the increase in curing time due to the

progress of cement hydration (Mamlouk and Zaniewski 2011) (Figs. 17 and 18).

Comparative analysis of the results shown in Figs. 7 and 8 indicates that the bonds between CPB particles cured to 2.5 h were weak to resist the shear stresses induced by the cyclic loading, while the shear resistance of the 4.0 h-CPB was higher due to stronger bonds between particles, which reduces the changes in acceleration and lateral displacement. Also, the bonds between the CPB particles cured to 10.0 h were high enough to resist the shear stress coming from the laminas and made the FLSB act as a rigid box. These facts strengthen the hypothesis that the CPB model cured to 2.5 h might be susceptible to cyclic loading-induced liquefaction, and the CPB material cured to 4.0 h and 10.0 h, is more resistant to liquefaction and ground movement.

### 4.3 Evolution the Pore Water Pressure, Effective Stress and Settlement

#### 4.3.1 Pore Water Pressure

Figure 9a–c exhibits the time-variation of pore water pressure (PWP) at different depths within the CPB models cured for 2.5 h (Fig. 9a), 4 h (Fig. 9b), and 10 h (Fig. 9c), respectively, before, during and after cyclic loading (i.e., from deposition time to about 24 h).

**4.3.1.1 Before Shaking** As can be seen in Fig. 9a, during the first 1 h (3600 s) after the disposal of the fresh CPB, there was first a rapid increase in the PWP in all depths of each CPB model. This progress in PWP is mainly related to the self-weight settlement and rearrangement of the tailings particles at the very early age, which decreases the volume of voids (Yilmaz et al. 2012). Subsequently, the PWP rapidly decreases due to the self-desiccation (Helinski et al. 2007; Ghirian and Fall 2014; Scrivener et al. 2015). The latter is experimentally supported by the suction monitoring results presented in Fig. 10 and discussed later. Moreover, the water evaporation should be considered as an additional factor in decreasing the PWP at shallow depths within the CPB samples.

**4.3.1.2 During Shaking** Prior to applying cyclic loads, hydrostatic (initial) conditions of the CPB

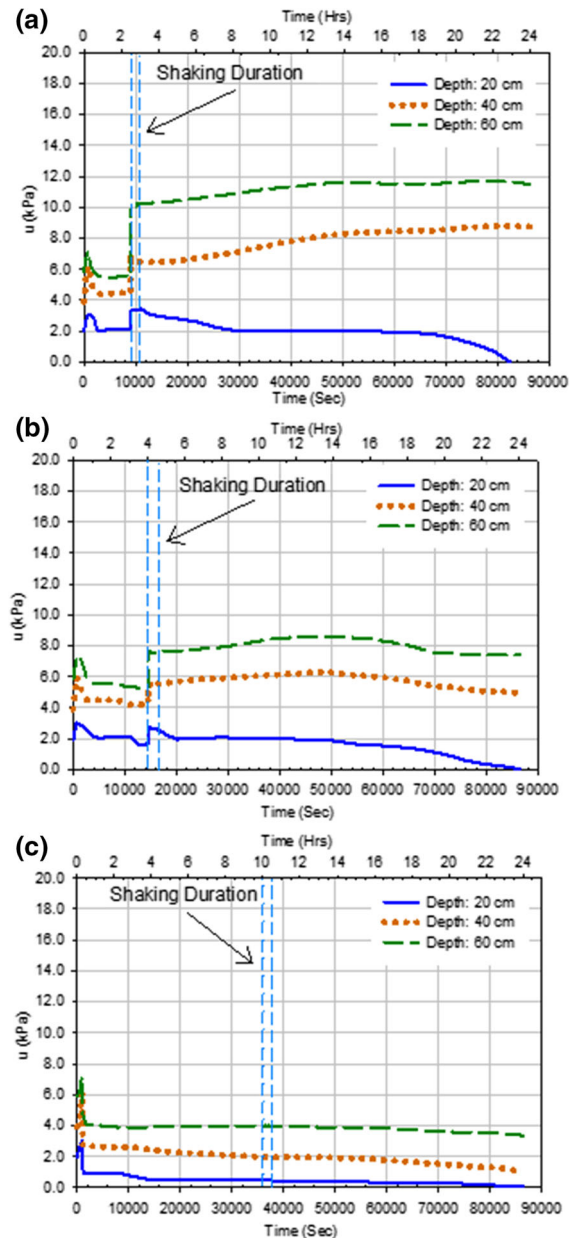


**Fig. 9** Pore water pressure histories at different depths vs times for CPB models cured to different times: **a** 2.5 h; **b** 4.0 h and **c** 10.0 h

material were determined. When shaking started, as expected, there was a quick increase in pore water pressure at all depths within the CPB materials cured to 2.5 h and 4.0 h until reaching peak values, while there was no rise in pore water pressure in the 10-h-old CPB. Moreover, as expected, this increase is bigger at greater depth. This buildup of pore water pressure is

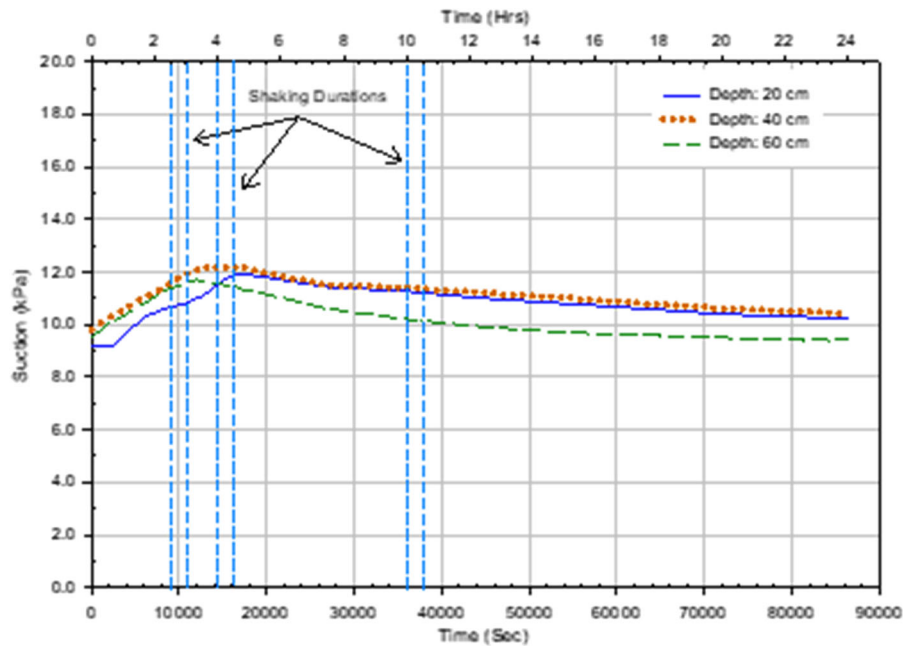


**Fig. 10** Suction evolution at different depths of the CPB model

related to the generation of excess pore water due to the contractive behavior of the saturated backfill material or particles (Bouckovalas et al. 2009; Saebimoghaddam 2010; Jefferies and Been 2015; Porcino et al. 2015) (Fig. 12; will be discussed below). However, the increase in pore water pressure within the CPB sample cured to 2.5 h was more significant than the increase in pore water pressure within the CPB sample cured to 4.0 h. This can be explained by the joint effect of the following factors: (i) the increase in water consumption by cement hydration (higher self-desiccation) as the curing time increases (i.e., progress of cement hydration) (Scrivener et al. 2015), and (ii) the precipitation of more cement hydration products as the curing time increases (Fig. 17 and 18), which in turn enhances the cementing bonds between the tailings grains (Saebimoghaddam 2010; Ghirian and Fall 2013; Scrivener et al. 2015), and thus reduces the contraction of the CPB materials (Fig. 12).

**4.3.1.3 After Shaking** After the end of shaking, the pore water pressure first slightly increased with time (i.e., regardless of the cement hydration progress) at the depths of 20 and 40 cm for the CPB models cured to 2.5 h and 4.0 h (with different magnitudes). This minimal rise in PWP at these depths was then followed

by a gradual reduction of the PWP until the end of the monitoring time. However, the PWP gradually decreased at the depth of 60 cm for the CPBs mentioned above after the end of shaking. This observed minimal increase in PWP at shallower depths (20 and 40 cm) may be explained by the contraction (settlement) of some tailings grains, which might have been partly in suspension at the end of the cycling loading. This contraction generated additional pore water pressure (Pépin et al. 2009). The aforementioned decrease of pore water pressure observed at all depths is mainly due to the self-desiccation (water consumption by cement hydration) (Ghirian and Fall 2013). However, at shallow depths (close to the CPB surface) of each sample, an additional factor contributes to the dissipation of the pore water pressure. This factor is the surface evaporation. Figures 9a–c show that the pore-water pressure at the shallow depth (20 cm) of each sample declined to less than the initial pore-water pressure. This phenomenon can be attributed to the combined effect of (i) self-desiccation due cement hydration (Ghirian and Fall 2013) and (ii) near surface evaporation due to the difference in relative humidity of the CPB surface and the ambient air (Abdul-Hussain and Fall 2012). This argument

regarding surface evaporation was experimentally confirmed in this study by determining the reduction in water content of a CPB material (prepared with the same mix components and conditions as the CPB used in this study) due to evaporation when exposed to environmental conditions (relative humidity, temperature) like those in which the shaking tests were performed. It was found that when the CPB sample is exposed to those conditions (temperature of 25 °C, and RH of 24%), about 60% of the water loss (reduction in CPB water content) near the surface of the CPB samples was related to evaporation.

### 4.3.2 Effective Stress

The evolution of effective vertical stresses at various depths during the shaking durations for CPB models cured (aged) for 2.5 h, 4 h, and 10 h, respectively, are shown in Fig. 11a–c. During shaking, these stresses decreased from their initial values in the samples cured to 2.5 h and 4.0 h. This decrease is due to the excess pore pressure development (Fig. 9a and b) as result of the contraction of CPB particles. However, in samples cured to 10.0 h, the effective stresses remain constant during shaking durations because there was no significant excess pore water pressure generation as shown and discussed previously (Fig. 9c).

### 4.3.3 Settlement (Vertical Displacement)

In this study, settlement (downward displacement) was recorded at various depths within the CPB models during shaking. This can reflect to the contractive behavior of the CPB particles and the increase in the backfill density (Ueng et al. 2006; Pépin et al. 2012b). Settlement time histories measured during the shaking at different depths within the CPB models cured (aged) for 2.5 h, 4.0 h, and 10 h, respectively, are shown in Fig. 12a–c. This figure depicts that the CPBs cured for 2.5 h and 4.0 h show significant settlement, whereas the CPB cured for 10 h shows negligible settlement (< 2 mm). This observed settlement indicates a contractive behaviour of the tailings particles (or volume change of the CPB) induced by the shaking. It can be also seen that the amount of settlement or contraction (volume change) within the CPB cured to 2.5 h was higher than its values in the backfill cured to 4.0 h and 10 h. This observation suggests that the longer the curing time or the higher

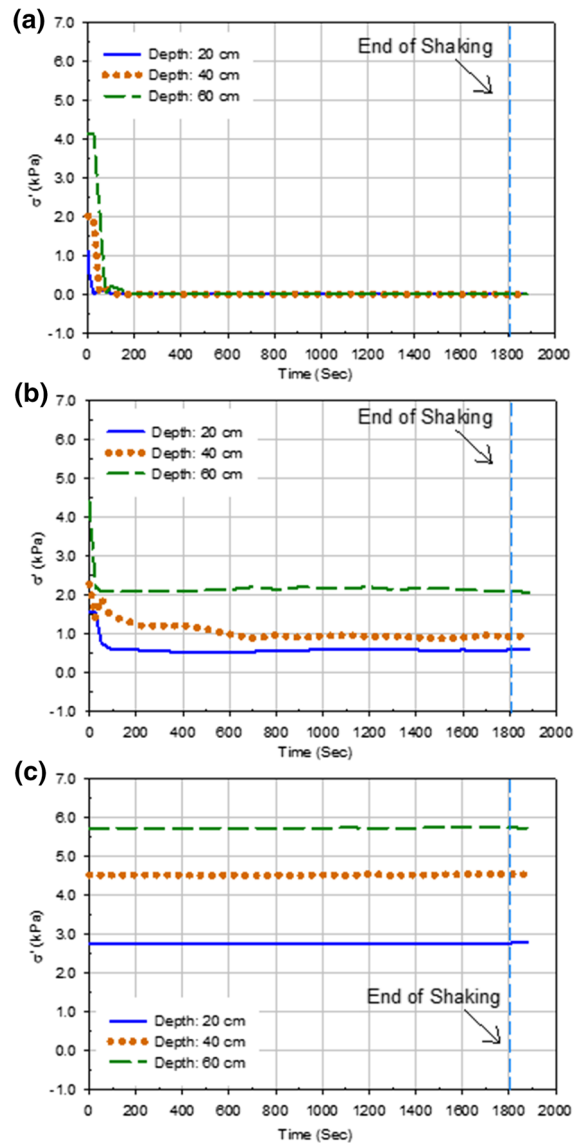


**Fig. 11** Effective stress at different depths vs times for CPB models cured to different times: **a** 2.5 h; **b** 4.0 h and **c** 10.0 h

cement hydration degree, the lesser the settlement induced by the shaking. This behavior, which is consistent with the results of PWP measurements and liquefaction analysis discussed in Sects. 4.2.1 and 4.3, respectively, is due to the fact that a greater cement hydration degree causes the precipitation of more cement hydration products (see Figs. 17–18), thereby increasing the density and strength of the CPB material (Fall et al. 2010; Scrivener et al. 2015). Consequently, the contracting behaviour or settlement of the CPB becomes smaller (Seed et al. 1975;

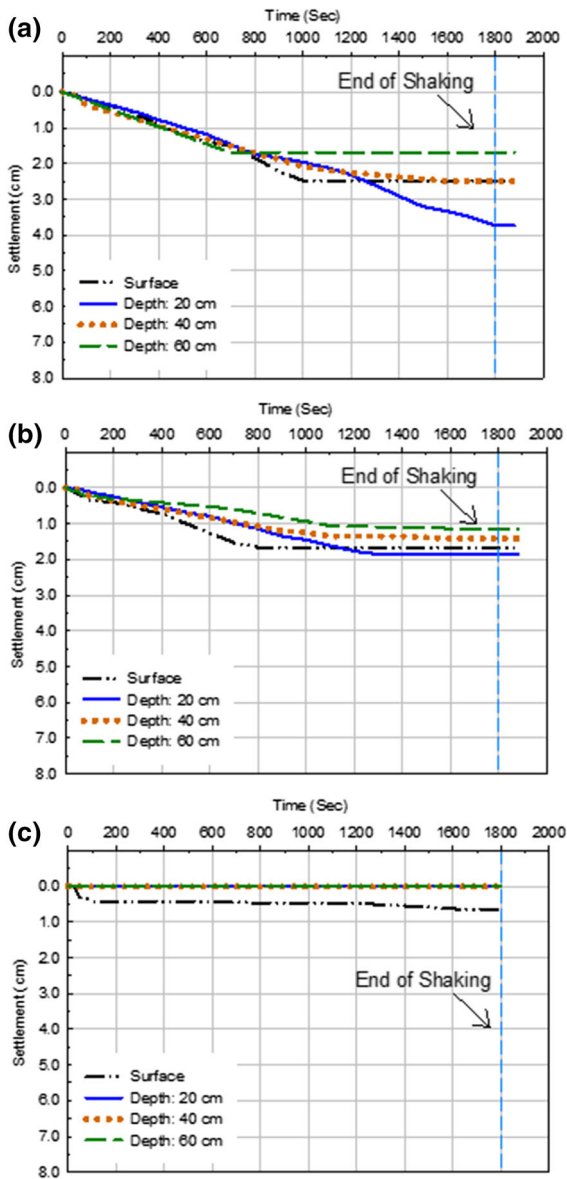


**Fig. 12** Settlement at different depths vs times for CPB models cured to different times during shaking: **a** 2.5 h; **b** 4.0 h and **c** 10.0 h

Tokimatsu and Seed 1987) during shaking. The settlement-depth variation of CPB cured for 2.5 h and 4.0 h can also be observed from Fig. 12. The settlement becomes smaller as the depth increases.

#### 4.4 Liquefaction Analysis

Numerous liquefaction triggering methods have been recommended and used to define or determine soil

liquefaction. These criteria include, strain/deformation-based liquefaction criteria, energy-based liquefaction criteria, (excess) pore ratio-based criteria, and strength-based criteria. Regardless of the advantages of these methods, there are some limitations, as detailed in various earlier studies (e.g., Wu et al. 2004). The excess pore-water pressure ratio ( $R_u$ ), which is the ratio between the excess pore-water pressure ( $\Delta u$ ) and the initial effective stress ( $\sigma'_o$ ), was used as the evaluation factor of soil liquefaction susceptibility. Liquefaction is generally defined as  $R_u = 1$ , while if  $R_u < 1$ , there is no liquefaction (Jiaer et al. 2004). The excess pore-water pressure criteria have been widely used in evaluating the liquefaction potential of soils or tailings in the laboratory, particularly in shaking table tests (Lu et al. 2019; Wang et al. 2019).

Figure 13a–c shows a comparison of the excess of PWP development (during shaking) at different depths and curing times for all CPB models. The excess of PWP in the CPBs cured to 2.5 h and 4.0 h varied with depth and shaking time, while there was no excess pore water pressure development during shaking within the CPB cured to 10.0 h. Figure 14a–c presents the pore-water pressure ratios determined during shaking of the CPB samples cured to 2.5 h, 4.0 h, and 10.0 h, respectively. It can be seen that CPB samples cured to 2.5 h are susceptible to liquefaction ( $R_u \geq 1$ ) under the applied cyclic loading conditions, while samples exposed to shaking after 4.0 and 10.0 h of curing were resistant to liquefaction ( $R_u < 1$ ). In other words, the more time that is given to cement to act, the less susceptible to cyclic loading-induced liquefaction the CPB will be. This increase of liquefaction resistance of CPB as the curing time increases is due to the coupled influence of the following two factors as discussed below: (i) production of more cement hydration products within the CPB pores due to progress of the cement hydration, which generates or enhances the cementation or cohesion between the tailings particles, and thus increasing the shear strength of the CPB material. The latter obviously results in the increase of the liquefaction resistance of the CPB; and (ii) the water consumption by the cement hydration (self-desiccation), and thus decreasing the pore water pressure or excess of pore pressure within the backfill. This is obviously associated with a rise of the effective stress



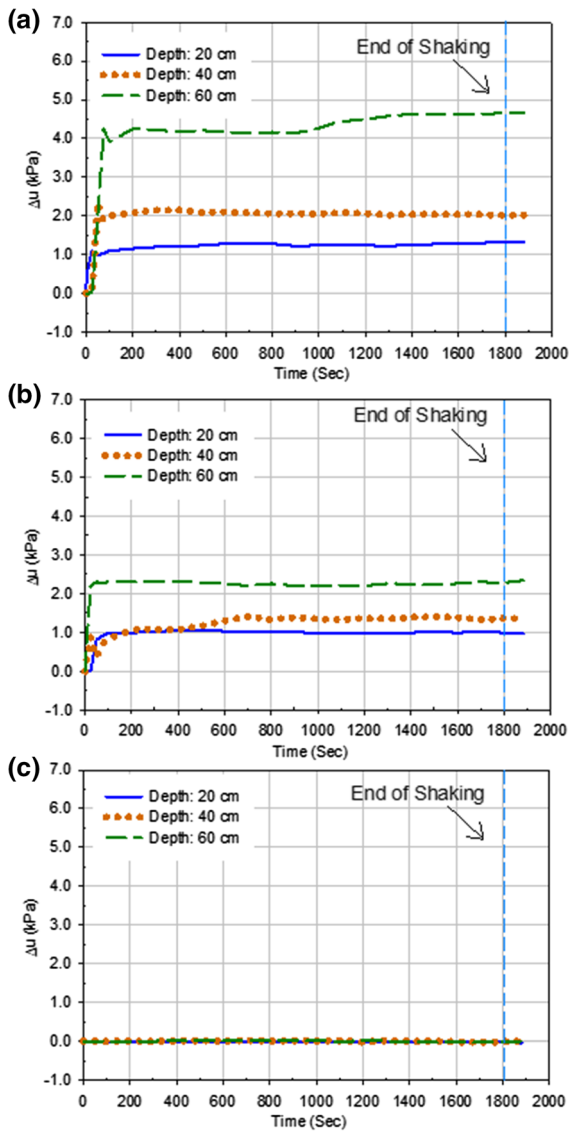


**Fig. 13** Excess pore water pressure ( $\Delta u$ ) development at different depths vs times for CPB models cured to different times: **a** 2.5 h; **b** 4.0 h and **c** 10.0 h

within the CPB, and consequently with an increase of the liquefaction resistance of the cementing backfill.

- (i) Production of more cement hydration products

The production of more cement hydration products as the curing time becomes longer is experimentally supported by the results of the microstructural analyses (thermal analysis (TG/DTG) and x-ray diffraction (XRD) analyses) performed on CPBs cured to

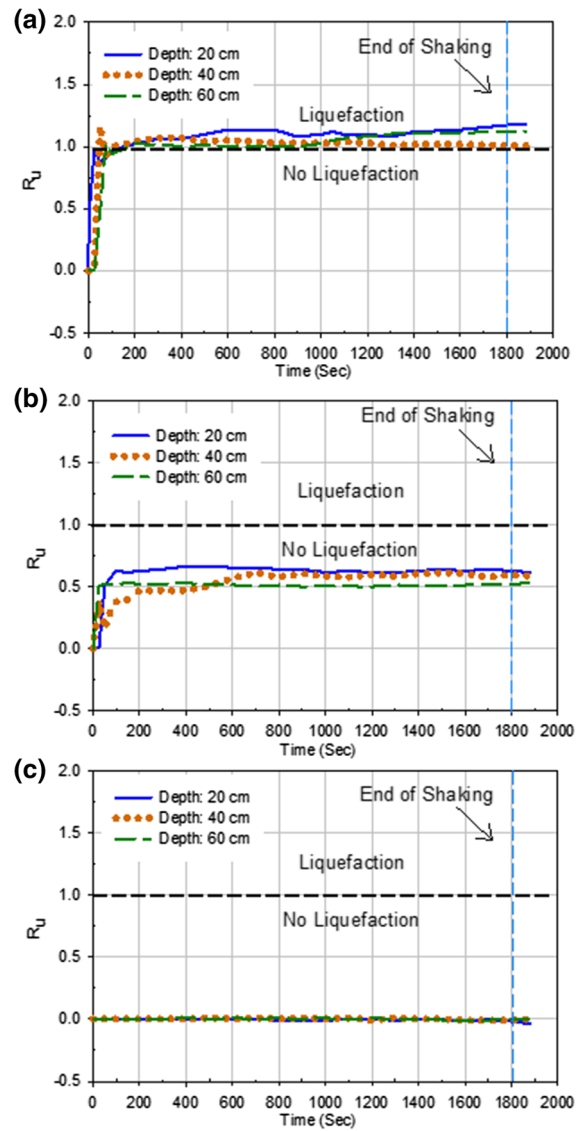


**Fig. 14** Pore -water pressure ratios determined at different depths vs times for CPB models cured to different times: **a** 2.5 h; **b** 4.0 h and **c** 10.0 h

different ages, 1 h and 4 h, (Figs. 17 and 18), respectively. From Fig. 17, it can be seen that the first peak (DTG) or modification in weight (TG) is found between 100 and 200 °C, which refers to the decomposition of the cement hydration products, such as ettringite, gypsum and C-S-H (Fall et al. 2010; Wang et al. 2016), while the second peak or weight change occurred at around 400–500 °C as a result of the disintegration of CH (Noumowé 1995; Zhou and Glasser 2001). Finally, the third peak or weight change

is observed between 600 and 700 °C due to the decomposition of the calcite (Noumowé 1995; Zhou and Glasser 2001; Fall et al. 2010; Haiqiang et al. 2016). Moreover, by comparing the TG/DTG diagrams of the CPB cured to 1.0 h and 4.0 h, it can be clearly noticed that the first and second peaks or weight changes are higher for CPB cured to 4.0 h, thus indicating that the amount of hydration products (such as CH and C-S-H) generated increases with a longer curing time. These thermal analysis results are consistent with the results of XRD analysis conducted on CPB samples cured to 1.0 h and 4.0 h, respectively, and presented in Fig. 18a, b. This figure shows the types and relative amounts of the cement hydration products (e.g., ettringite, gypsum, CH, C-S-H) formed within the CPB samples. It is observed that some of these products have a higher intensity in the CPB sample cured for 4.0 h. In other words, more hydration products were formed in the older than the younger sample. For instance, the intensity of the ettringite at  $9^\circ - 2\theta$  is 260 CPS and 300 CPS in the case of CPB samples cured to 1.0 h and 4.0 h, respectively. Similarly, the ettringite intensity at  $22^\circ - 2\theta$  is 160 CPS and 200 CPS in the case of CPB samples cured to 1.0 h and 4.0 h, respectively.

Figures 15 and 16, which depict the results of the monitoring of the time-dependent evolution of the temperature and EC at different depths of the CPB models, respectively, show that the cement hydration rate (or progress), in other words, the magnitude of cement hydrations formed within the CPB, is quite similar at all depths of the CPBs. Indeed, these figures show that there is almost an overlap of the time-dependent evolution curves of the temperature and EC at all depths. Moreover, the time required to reach the peak values of EC is similar for all depths. The initial increase of the EC up to the peak value (Fig. 16) is due to an increase of the concentration of ions in the CPB pore water solution because of the dissolution of cement grains. The observed decrease of the EC after the peak value results from the combined effects of the following factors: (a) start of the development of cement hydration products, (b) decrease of the free water, and (c) refinement and subdivision of the capillary pores (Salem and Ragai 2001; Courard et al. 2014) (Figs. 17, 18).

#### (ii) Self-desiccation of CPB

Self-desiccation of cementitious material, a mechanism caused by cement hydration, can be simply described as the reduction of net total volume of water

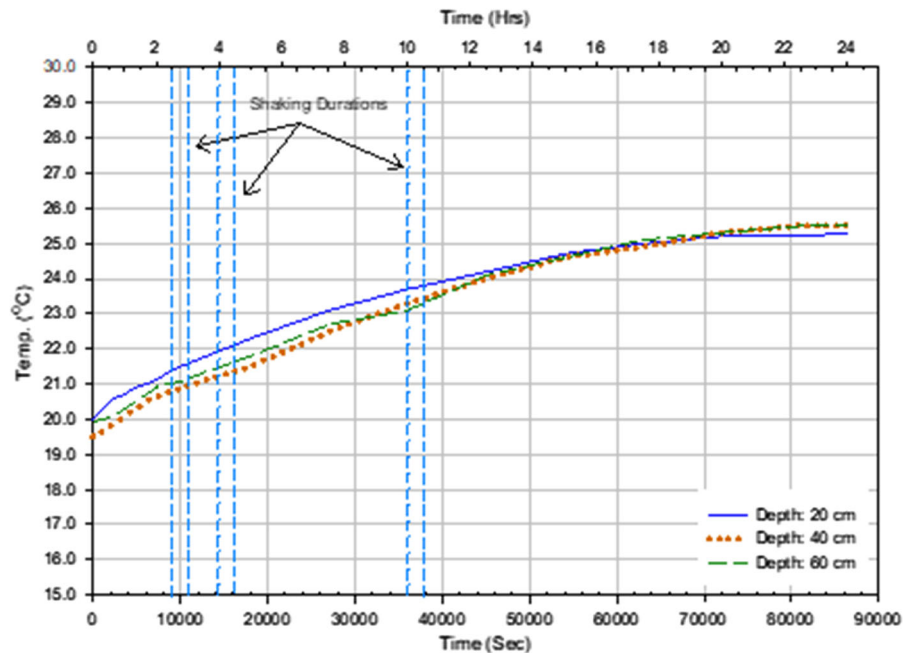


**Fig. 15** Evolution of hydration heat with curing time within CPB models

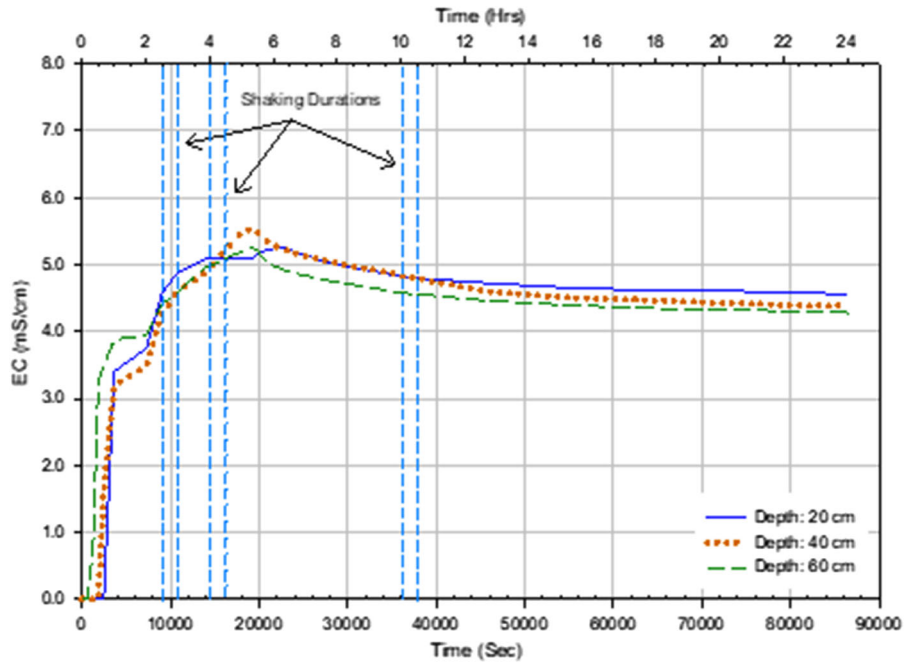


**Fig. 16** Electrical Conductivity at different depths of the CPB models

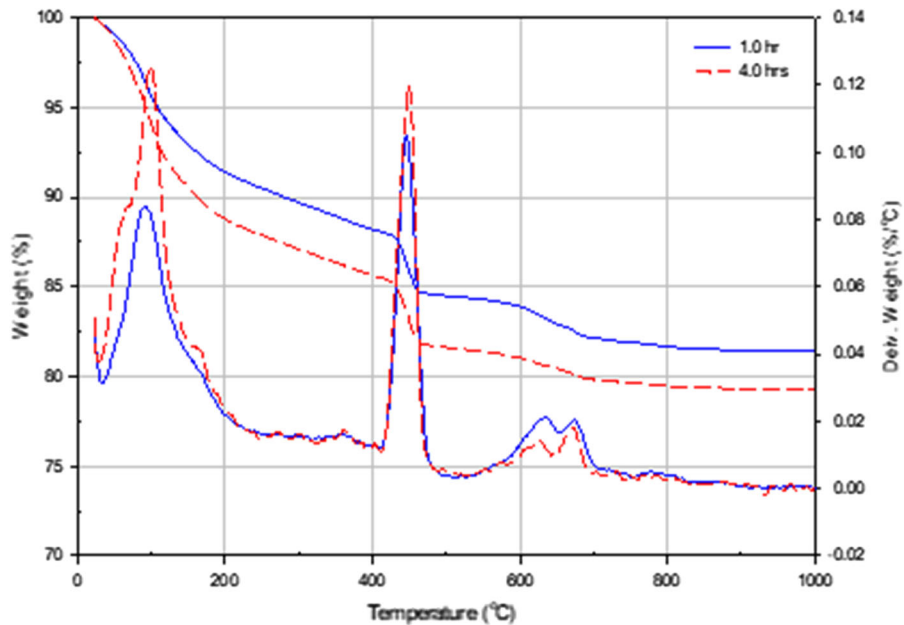


**Fig. 17** Effect of curing time on TG/DTG diagrams for CPB cured to 1.0 h and 4.0 h

and solid particles or total volume of the material as a result of the process of cement hydration (Li and Fall 2016), leading to a reduction in PWP and/or a generation of negative pore water pressure (suction) (Ghirian and Fall 2013). Accordingly, the effective

stress and strength of these materials increase as self-desiccation takes place (Abdul-Hussain and Fall 2012; Fredlund et al. 2012; Ghirian and Fall 2014). Figures 19 and 10, which show the evolution of the volumetric water content (VWC) and suction in the

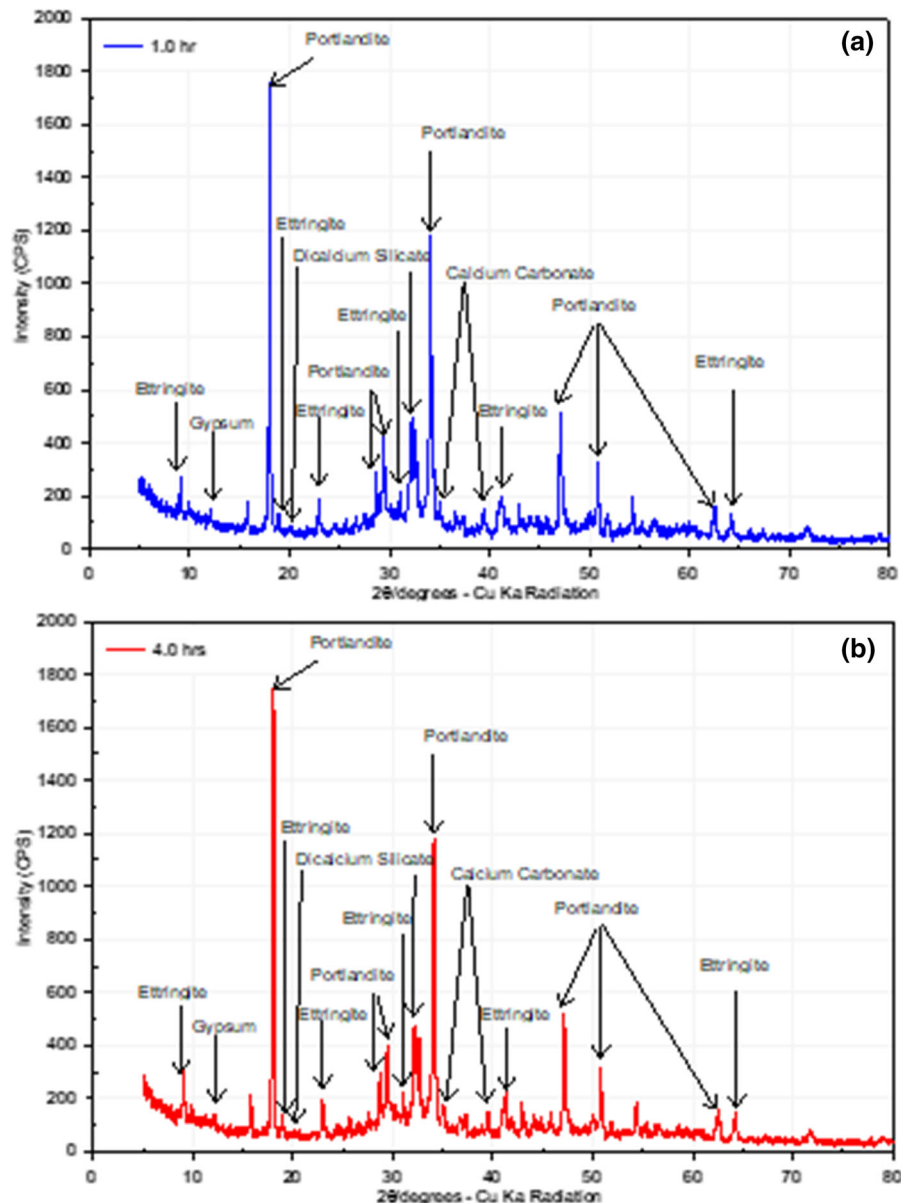


**Fig. 18** Effect of curing time on the XRD result of CPB cured to: **a** 1.0 h; **b** 4.0 h

CPB at different depths, respectively, support the fact that self-desiccation did take place in the CPB. A gradual increase in the volumetric water content (VWC) in the first hours at all depths of the CPB material can be observed in Fig. 19. The peak values of VWC were reached after 6 h. Afterward, it experienced a slight decrease and became relatively constant till the completion of the monitoring time. This increase in VWC is related to the decrease of the total volume of the CPB due to the self-desiccation

since the VWC expresses the ratio of volume of water to the total volume of the soil. Moreover, the amount of water or water content decreased during this period of time as evidenced by the suction measurements results presented in Fig. 10. It should be recalled that, as mentioned in the Sect. 2.3, the suction sensor (ECH2-MPS6) used has a measurement accuracy of  $\pm 10\%$  of reading + 2 kPa, from 9 to 100 kPa. Thus, considering the low values of suction obtained (Fig. 10) and these suction sensor measurement

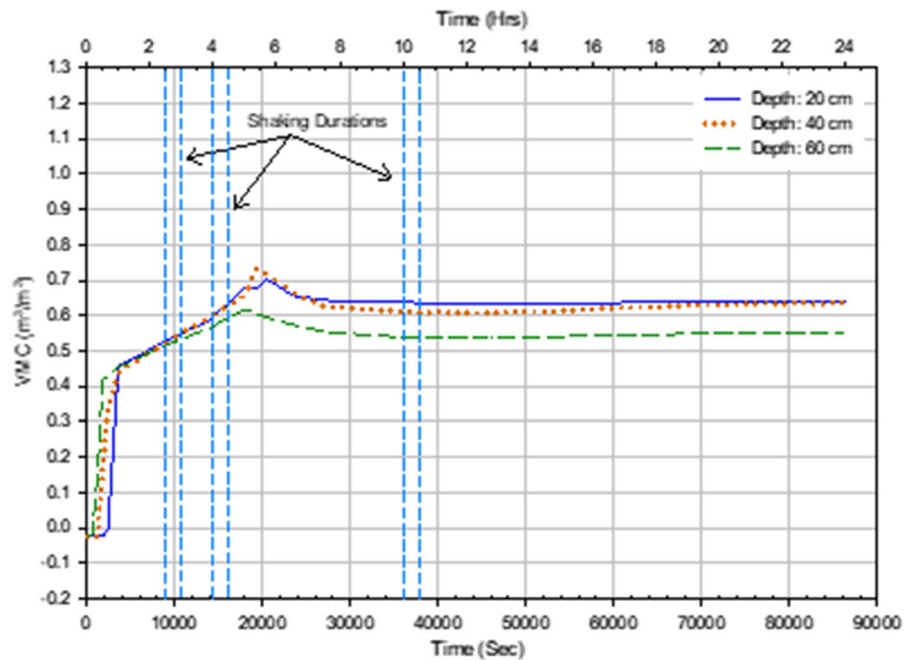


**Fig. 19** Change in volumetric water content at different depths of the CPB models

limitations, the evolution of the suction presented in Fig. 10, although useful and consistent with the degrees of saturation of the CPB, should be considered as qualitative. This figure shows a very small suction has developed in the CPB shortly after its disposal into the laminar shear box. Then, the suction value increased until reaching its peak after 6 h. Afterward, the suction decreased slightly and then remained relatively constant until the end of the monitoring. This generation of small suction and its increase can be explained by the fact that the chemical reactions of the cement hydration result in the consumption of water in the capillary pores of CPB (Wang et al. 2016), which decreases the water content in the hydrating backfill. The reduction of water content in the backfill or soil allows air to enter the pores between tailings or soil particles and thus generate air bubbles. Consequently, this turns the backfill or soil from saturated condition to partially saturated conditions (Fredlund et al. 2012). This effect was experimentally confirmed in this study, as it was noted that the degree of saturation decreased from 100% (immediately after casting) to around 94–96% (after about 2 h). This reduction in water content leads to a decrease of the pore water

pressure, in other words to an increase of the effective stress, and thus to an increase of the liquefaction resistance of the CPB. Moreover, the presence of air bubbles inside the pores of a soil will enhance its liquefaction resistance, because the air can absorb the generated excess PWP by reducing its volume (Okamura and Soga 2006).

## 5 Summary and Conclusion

This manuscript has evaluated and discussed the geotechnical response (e.g., deformation, excess of pore water pressure, effective stress, liquefaction potential) of paste backfill undergoing cementation to cyclic loadings by using the shaking table testing technique. This assessment was conducted by applying cyclic loading on paste backfill models cured at different times (2.5 h, 4.0 h and 10.0 h), which were casted in a flexible laminar shear box. The paste backfill models were also instrumented with numerous sets of sensors and transducers to monitor the evolution of several parameters (pore water pressure, suction, lateral and horizontal displacement,

acceleration, temperature, electrical conductivity) before, during and after shaking. The obtained results show that the acceleration, horizontal and vertical displacement and excess pore water pressure of the CPB under cyclic loading are significantly affected by the curing time or the degree of cement hydration and the depth in the CPB. It is also found that the cyclic loading has no significant influence on the progress of the cementation hydration. Moreover, young (2.5 h old) CPB material can be susceptible to liquefaction, whereas older CPBs (curing time  $\geq 4$  h) are resistant to liquefaction under the studied cyclic conditions. This resistance to liquefaction is due to the combined effect of two factors: (i) the strengthening of the cementation between the soil (tailings) particles, which increases the shear resistance of the CPB material; (ii) the self-desiccation, which decreases the pore water pressure or leads to the development of suction (due to generation of air bulbs) within the backfill, and thus increasing of the effective stress in the CPB. The extent of these effects depends on the curing time, and it increases for a longer curing time. These relatively large-scale 1-g tests on CPB are time consuming and expensive; however, they have facilitated a better understanding of the cyclic behaviour and liquefaction potential of CPB at early ages as well as provided information and data that are useful for liquefaction assessment of CPB structures, and also for future development of constitutive models to describe and predict the cyclic behaviour of hydrating paste backfill or soil undergoing cementation.

**Acknowledgements** The authors would like to thank the National Natural Sciences and Engineering Research Council of Canada (NSERC) for financially supporting this project. Moreover, the authors would like to thank Dr. Mohammed Al-Umar, Dr. Gamal Elnabelsya, and Dr. Mohamed Salah for their help with the experimental tests.

**Funding** National Natural Sciences and Engineering Research Council of Canada (NSERC).

**Availability of Data and Material** All data and materials or used during the study appear in the submitted article.

#### Declarations

**Conflict of interest** There are no known conflicts of interests or competing interests.

**Code Availability** Not applicable.

## References

- Abdul-Hussain N, Fall M (2012) Thermo-hydro-mechanical behaviour of sodium silicate-cemented paste tailings in column experiments. *Tunn Undergr Space Technol* 29:85–93
- Acar YB, El-Tahir ETA (1986) Low strain dynamic properties of artificially cemented sand. *J Geotech Eng* 112(11):1001–1015
- Alainachi I, Fall M (2021a) Chemically induced changes in the geotechnical response of cementing paste backfill in shaking table test. *J Rock Mech Geotech Eng* 13:513
- Alainachi, I., Fall, M. (2021b). Temperature induced changes in the behaviour of cementing fine-grained soils under dynamic loadings. *Geomech Geoenviron Eng*, 1–19.
- Aldhafeeri Z, Fall M (2016) Time and damage induced changes in the chemical reactivity of cemented paste backfill. *J Environ Chem Eng* 4(4):4038–4049
- Anastasopoulos I, Georgarakos T, Georgiannou V, Drosos V, Kourkoulis R (2010) Seismic performance of bar-mat reinforced-soil retaining wall: shaking table testing versus numerical analysis with modified kinematic hardening constitutive model. *Soil Dyn Earthq Eng* 30(10):1089–1105
- ASTM C143/C143M-15a (2015). “Standard test method for slump of hydraulic-cement concrete,”
- Atkinson GM, Kaka SI, Eaton D, Bent A, Peci V, Halchuk S (2008) A very close look at a moderate earthquake near Sudbury, Ontario. *Seismol Res Lett* 79(1):119–131
- Bairro R and Vaz C (2000) *Shaking table testing of civil engineering structures-The LNEC 3D simulator experience*, translated by Auckland, New Zealand.
- Becker D, Cailleau B, Kaiser D, Dahm T (2014) Macroscopic failure processes at mines revealed by acoustic emission (AE) monitoring. *Bull Seismol Soc Am* 104(4):1785–1801
- Bouckovalas GD, Papadimitriou AG, Niarchos D (2009) Gravel drains for the remediation of liquefiable sites: the seed & booker (1977) approach revisited. International conference on performance-based design. Japan, International society for soil mechanics and geotechnical engineering, Tokyo, pp 61–75
- Bullard JW, Jennings HM, Livingston RA, Nonat A, Scherer GW, Schweitzer JS, Scrivener KL, Thomas JJ (2011) Mechanisms of cement hydration. *Cement Concr Res* 41(12):1208–1223
- Carraro JAH, Prezzi M, Salgado R (2009) Shear strength and stiffness of sands containing plastic or nonplastic fines. *J Geotech Geoenviron Eng* 135(9):1167–1178
- Carter DP (1988) Liquefaction potential of sand deposits under low levels of excitation. California Univ, Berkeley, CA, USA
- Chopra AK (2005). *Earthquake dynamics of structures—a primer*. Earthquake Engineering Research Institute (EERI), USA.
- Chou H, Yang C, Hsieh B, Chang S (2001) A study of liquefaction related damages on shield tunnels. *Tunn Undergr Space Technol* 16:185–193
- Courard L, Michel F, Perkowicz S, Garbacz A (2014) Effects of limestone fillers on surface free energy and electrical

- conductivity of the interstitial solution of cement mixes. *Cement Concr Compos* 45:111–116
- Cui L, Fall M (2015) A coupled thermo-hydro-mechanical-chemical model for underground cemented paste backfill. *Tunn Undergr Space Technol* 50:396–414
- Cui L, Fall M (2017) Modeling of pressure on retaining structures for fill mass. *Tunn Undergr Space Technol* 69:94–107
- Douglas J (2003) Earthquake ground motion estimation using strong-motion records: a review of equations for the estimation of peak ground acceleration and response spectral ordinates. *Earth Sci Rev* 61(1–2):43–104
- Dungca JR, Kuwano J, Takahashi A, Saruwatari T, Izawa J, Suzuki H, Tokimatsu K (2006) Shaking table tests on the lateral response of a pile buried in liquefied sand. *Soil Dyn Earthq Eng* 26(2–4):287–295
- Plewes HD, Chambers RW, Friedel R, Jibiki TK, Sy A (2010) Ground improvement by dynamic compaction at a tailings disposal facility *International conference on recent advances in geotechnical earthquake engineering and soil dynamics 2*, Missouri University of Science and Technology
- Fall M, Benzaazoua M, Ouellet S (2005) Experimental characterization of the influence of tailings fineness and density on the quality of cemented paste backfill. *Miner Eng* 18(1):41–44
- Fall M, Benzaazoua M, Sae E (2008) Mix proportioning of underground cemented paste backfill. *J Tunn Undergr Space* 23:80–90
- Fall M, Célestin JC, Pokharel M, Touré M (2010) A contribution to understanding the effects of curing temperature on the mechanical properties of mine cemented tailings backfill. *Eng Geol* 114(3–4):397–413
- Fang K, Fall M (2020) Shear behavior of the interface between rock and cemented backfill: effect of curing stress, drainage condition and backfilling rate. *Rock Mech Rock Eng* 53(1):325–336
- Fredlund DG, Rahardjo H, Fredlund MD (2012) *Unsaturated soil mechanics in engineering practice*. John Wiley & Sons, Hoboken, New Jersey, USA
- Ghirian A, Fall M (2013) Coupled thermo-hydro-mechanical-chemical behaviour of cemented paste backfill in column experiments. Part I: physical, hydraulic and thermal processes and characteristics. *Eng Geol* 164:195–207
- Ghirian A, Fall M (2014) Coupled thermo-hydro-mechanical-chemical behaviour of cemented paste backfill in column experiments. *Eng Geol* 170:11–23
- Ghirian A, Fall M (2016) Long-term coupled behaviour of cemented paste backfill in load cell experiments. *Geomech Geoen* 11(4):237–251
- Guoxing C, Su C, Xi Z, Xiuli D, Chengzhi QI, Zhihua W (2015) Shaking-table tests and numerical simulations on a subway structure in soft soil. *Soil Dyn Earthq Eng* 76:13–28
- Haiqiang J, Fall M, Cui L (2016) Yield stress of cemented paste backfill in sub-zero environments: experimental results. *Miner Eng* 92:141–150
- Hasegawa HS, Wetmiller RJ, Gendzwill DJ (1989) Induced seismicity in mines in Canada—an overview. *Pure Appl Geophys* 129(3–4):423–453
- Hasegawa A, Nakajima J, Uchida N, Okada T, Zhao D, Matsuzawa T, Umino N (2009) Plate subduction, and generation of earthquakes and magmas in Japan as inferred from seismic observations: an overview. *Gondwana Res* 16(3–4):370–400
- Helinski M, Fourie A, Fahey M, Ismail M (2007) Assessment of the self-desiccation process in cemented mine backfills. *Can Geotech J* 44(10):1148–1156
- Iai S (1989) Similitude for shaking table tests on soil-structure-fluid model in 1-g gravitational field. *Soils Found* 29(1):105–118
- Ishihara K (1996) *Soil behavior in earthquake geotechnics*. Oxford University Press, NY, USA
- Jamali M (2012) *Effect of binder content and load history on the one dimensional compression of Williams Mine cemented paste backfill*, Master of applied science Thesis, University of Toronto.
- James M, Jolette D, Aubertin M and Bussière B (2003) *An experimental set-up to investigate tailings liquefaction and control measures*, translated by Montréal, QC, Canada.
- Jefferies M, Been K (2015) *Soil liquefaction: a critical state approach*, 2nd edn. Taylor & Francis, London, UK
- Jiaer WU, Kammerer AM, Riemer MF, Seed RB and Pestana JM (2004) *Laboratory study of liquefaction triggering criteria*, translated by Vancouver, BC, Canada.
- Kesimal A, Yilmaz E, Ercikdi B, Alp I, Devenci H (2005) Effect of properties of tailings and binder on the short-and long-term strength and stability of cemented paste backfill. *Mater Lett* 59(28):3703–3709
- Li L, Aubertin M (2012) A modified solution to assess the required strength of exposed backfill in mine stopes. *Can Geotech J* 49(8):994–1002
- Li W, Fall M (2016) Sulphate effect on the early age strength and self-desiccation of cemented paste backfill. *Constr Build Mater* 106:296–304
- Lu G, Fall M (2017) Simulation of blast induced liquefaction susceptibility of subsurface fill mass. *Geotech Geol Eng* 36(3):1683–1706
- Lu G, Fall M, Yang Z (2019) An evolutive bounding surface plasticity model for early-age cemented tailings backfill under cyclic loading. *Soil Dyn Earthq Eng* 117:339–356
- Mamlouk MS, Zaniewski JP (2011) *Materials for civil and construction engineers*, 3rd edn. Pearson Prentice Hall, Upper Saddle River, New Jersey
- Meymand PJ (1998) *Shaking table scale model Tests of non-linear soil-pile-superstructure interaction in soft clay*, PhD dissertation. U.C, Berkeley
- Mohamed FMO (2014) *Bearing capacity and settlement behaviour of footings subjected to static and seismic loading conditions in unsaturated sandy soils*, Ph.D. Thesis, University of Ottawa.
- Moncarz PD and Krawinkler H (1981) *Theory and application of experimental model analysis in earthquake engineering*, Stanford University.
- Motamed R, Towhata I, Honda T, Tabata K, Abe A (2013) Pile group response to liquefaction-induced lateral spreading: E-defense large shake table test. *Soil Dyn Earthq Eng* 51:35–46
- Nasir O, Fall M (2010) Coupling binder hydration, temperature and compressive strength development of underground cemented paste backfill at early ages. *Tunn Undergr Space Technol* 25(1):9–20

- Natural Resources Canada (2019). Earthquake reports for 2019. [online], available: <http://www.seismescanada.nrcan.gc.ca/recent/2019/index-en.php> 2019].
- Ngadimon K (2006) *Design and simulation of hydraulic shaking table*, Ph.D. Thesis, University of Technology.
- Noumowé A (1995) *Effet des hautes températures (20°C–600°C) sur le béton*, Ph.D. Thesis, Institut National des Sciences Appliquées.
- Nouri H, Fakher A, Jones C (2006) Development of horizontal slice method for seismic stability analysis of reinforced slopes and walls. *Geotext Geomembr* 24(3):175–187
- Nouri H, Fakher A, Jones CJFP (2008) Evaluating the effects of the magnitude and amplification of pseudo-static acceleration on reinforced soil slopes and walls using the limit equilibrium horizontal slices method. *Geotext Geomembr* 26(3):263–278
- Nuttl OW (1973) Seismic wave attenuation and magnitude relations for eastern North America. *J Geophys Res* 78(5):876–885
- Okamura M, Soga Y (2006) Effect of pore fluid compressibility on liquefaction resistance of partially saturated sand. *Soils Found* 46(5):695–700
- Ontario Mining Association (2017). *Ontario Mineral Production*.
- Özgen S, Malkoç Ö, Doğancık C, Sabah E, Şapçı FO (2011) Optimization of a multi gravity separator to produce clean coal from Turkish lignite fine coal tailings. *Fuel* 90(4):1549–1555
- Pépin N, Aubertin M, James M, Leclerc M (2012b) Seismic simulator testing to investigate the cyclic behavior of tailings in an instrumented rigid box. *Geotech Test J* 35(3):469–479
- Pépin N, Aubertin M and James M (2009) *An investigation of the cyclic behaviour of tailings using shaking table tests—effect of a drainage inclusion on porewater development*, translated by Halifax, N.S., Canada.
- Pépin N, Aubertin M, James M (2012a) Seismic table investigation of the effect of inclusions on the cyclic behaviour of tailings. *Can Geotech J* 49(4):416–426
- Porcino D, Marciandò V, Granata R (2015) Cyclic liquefaction behaviour of a moderately cemented grouted sand under repeated loading. *Soil Dyn Earthq Eng* 79:36–46
- Poulos SJ, Robinsky EI, Keller TO (1985) Liquefaction resistance of thickened tailings. *J Geotech Eng* 111(12):1380–1394
- Saebimoghaddam A (2010) *Liquefaction of early age cemented paste backfill*, Ph.D Thesis, University of Toronto.
- Salem TM, Ragai SM (2001) Electrical conductivity of granulated slag-cement kiln dust-silica fume pastes at different porosities. *Cem Concr Res* 31(5):781–787
- Scrivener KL, Juilland P, Monteiro PJM (2015) Advances in understanding hydration of Portland cement. *Cem Concr Res* 78:38–56
- Seed HB, Pyke R, Martin GR (1975) Effect of multi-directional shaking on liquefaction of sands. University of California, Earthquake engineering research Center
- Srilatha N, Madhavi Latha G, Puttappa CG (2013) Effect of frequency on seismic response of reinforced soil slopes in shaking table tests. *Geotext Geomembr* 36:27–32
- Sriskandakumar S (2004). *Cyclic loading response of fraser river sand for validation of numerical models simulating centrifuge tests*, Ph.D Thesis, University of British Columbia, Canada.
- Su C, Baizan T, Zhao K, Xiaojn L, Haiyang Z (2020) Seismic response of irregular underground structures under adverse soil conditions using shaking table tests. *Tunn Undergr Space Technol* 95:103145
- Sudarshan NM, Chandrashekar Rao T (2017) Vibration impact on fresh concrete of conventional and UHPFRC. *Int J Appl Eng Res* 12(8):1683–1690
- Takahashi A, Takemura J, Suzuki A, Kusakabe O (2001) Development and performance of an active type shear box in a centrifuge. *Int J Phy Model Geotech* 1(2):1–17
- Thompson BD, Grabinsky MW, Bowden WF and Counter DB (2009). *In-situ measurements of cemented paste backfill in long-hole stope*, translated by Toronto, ON, Canada.
- Tokimatsu K, Seed HB (1987) Evaluation of settlements in sands due to earthquake shaking. *J Geotech Eng* 113(8):861–878
- Tuttle M, Law KT, Seeber L, Jacob K (1990) Liquefaction and ground failure induced by the 1988 Saguenay, Quebec, earthquake. *Can Geotech J* 27(5):580–589
- Ueng TS, Wang MH, Chen MH, Chen CH, Peng LH (2006) A large biaxial shear box for shaking table test on saturated sand. *Geotech Test J* 29(1):1–8
- Wang L, Chen G, Chen S (2015) Experimental study on seismic response of geogrid reinforced rigid retaining walls with saturated backfill sand. *Geotext Geomembr* 43(1):35–45
- Wang Y, Fall M, Wu A (2016) Initial temperature-dependence of strength development and self-desiccation in cemented paste backfill that contains sodium silicate. *Cement Concr Compos* 67:101–110
- Wang J, Salam S, Xiao M (2019) The effect of shaking history on liquefaction resistance of sand deposit using shake table testing. In *Geo-congress 2019: earthquake engineering and soil dynamics*. American Society of Civil Engineers, Reston, VA, USA, pp. 285–293
- Wu D, Fall M, Cai S (2014) Numerical modelling of thermally and hydraulically coupled processes in hydrating cemented tailings backfill columns. *Int J Min Reclam Environ* 28(3):173–199
- Wu J, Kammerer AM, Riemer MF, Seed RB, Pestana JM (2004). Laboratory study of liquefaction triggering criteria. In: *13th world conference on earthquake engineering, Vancouver, B.C., Canada*, paper No 2580.
- Yang L, Woods RD (2015) Shear stiffness modeling of cemented clay. *Can Geotech J* 52(2):156–166
- Yilmaz E, Belem T, Benzaazoua M (2012) One-dimensional consolidation parameters of cemented paste backfills/parametry jednowymiarowej konsolidacji podsadzki w postaci Cementowej Pasty. *Gospodarka Surowcami Mineralnymi—mineral Resour Manag* 28(4):29–45
- Yilmaz E, Belem T, Bussière B, Mbonimpa M, Benzaazoua M (2015) Curing time effect on consolidation behaviour of cemented paste backfill containing different cement types and contents. *Constr Build Mater* 75:99–111
- Zheng Y, Yue C (2020) Shaking table test study on the functionality of rubber isolation bearing used in underground structure subjected to earthquakes. *Tunn Undergr Space Technol* 98:103153



- Zhou Q, Glasser FP (2001) Thermal stability and decomposition mechanisms of ettringite at  $<120^{\circ}\text{C}$ . *Cem Concr Res* 31(9):1333–1339
- Zhu F, Clark JI (1994) The effect of dynamic loading on lateral stress in sand. *Can Geotech J* 31(2):308–311

**Publisher's Note** Springer Nature remains neutral with regard to jurisdictional claims in published maps and institutional affiliations.